Surface Characterization of Polythiophene:Fullerene Blends on Different Electrodes Using Near Edge X-ray Absorption Fine Structure

ARTICLE *in* ACS APPLIED MATERIALS & INTERFACES · MARCH 2011

Impact Factor: 6.72 · DOI: 10.1021/am101055r · Source: PubMed

11 AUTHORS, INCLUDING:

Andreas F Tillack
University of Washington Seattle
8 PUBLICATIONS **180** CITATIONS
SEE PROFILE

Dennis Nordlund
Stanford University
188 PUBLICATIONS **4,627** CITATIONS
SEE PROFILE

Hin-Lap Yip
South China University of Technology
123 PUBLICATIONS **6,896** CITATIONS
SEE PROFILE

Alex K-Y Jen
University of Washington Seattle
391 PUBLICATIONS **15,978** CITATIONS
SEE PROFILE

ACS APPLIED MATERIALS & INTERFACES

RESEARCH ARTICLE

www.acsami.org

Surface Characterization of Polythiophene:Fullerene Blends on Different Electrodes Using Near Edge X-ray Absorption Fine Structure

Andreas F. Tillack,[†] Kevin M. Noone,[†] Bradley A. MacLeod,[†] Dennis Nordlund,[‡] Kenneth P. Nagle,[§] Joseph A. Bradley,[§] Steven K. Hau,[⊥] Hin-Lap Yip,[⊥,¶] Alex K.-Y. Jen,[⊥,¶] Gerald T. Seidler,[§] and David S. Ginger*[,†]

[†]Department of Chemistry, University of Washington, Seattle, Washington 98195-1700, United States

[‡]Stanford Synchrotron Radiation Laboratory, 2575 Sand Hill Road MS69, Menlo Park, California 94025, United States

[§]Department of Physics, University of Washington, Seattle, Washington 98195-1560, United States

[⊥]Department of Materials Science and Engineering and [¶]Institute of Advanced Materials and Technology, University of Washington, Seattle, Washington 98195-2120, United States

Supporting Information

ABSTRACT: We study the top surface composition of blends of the conjugated polymer regioregular poly-3-hexylthiophene (P3HT) with the fullerene (6,6)-phenyl-C_{61}-butyric acid methyl ester (PCBM), an important model system for organic photovoltaics (OPVs), using near-edge X-ray absorption fine structure spectroscopy (NEXAFS). We compare the ratio of P3HT to PCBM near the air/film interface that results from preparing blend films on two sets of substrates: (1) poly(3,4-ethylenedioxythiophene) poly(styrenesulfonate) (PEDOT:PSS) coated indium tin oxide (ITO) as is commonly used in conventional OPV structures and (2) ZnO substrates that are either unmodified or modified with a C_{60}-like self-assembled monolayer, similar to those that have been recently reported in inverted OPV structures. We find that the top surface (the film/air interface) is enriched in P3HT compared to the bulk, regardless of substrate or annealing conditions, indicating that changes in device performance due to substrate modification treatments should be attributed to the buried substrate/film interface and the bulk of the film rather than the exposed film/air interface.

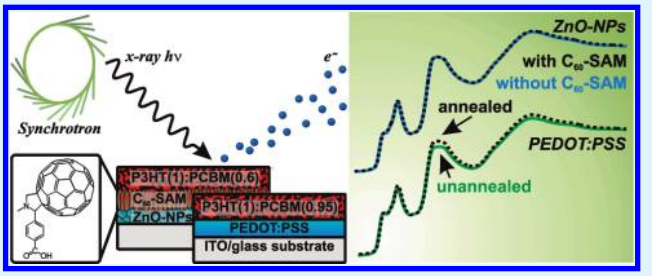

KEYWORDS: NEXAFS, P3HT, PCBM, top surface composition, wetting layer, vertical composition, polymer solar cell, PCBM density, vertical phase segregation

Organic bulk-heterojunction solar cells based on blends of regioregular poly-3-hexylthiophene (P3HT) and (6,6)-phenyl-C_{61}-butyric acid methyl ester (PCBM) are important model systems for understanding processing/performance correlations in organic photovoltaics. Both the surface composition and molecular orientation of the top few nanometers of the blended organic semiconductor film influence how materials processing parameters affect device performance.[1,2] For instance, the orientation of the surface layer may affect the electronic coupling between the top contact and the semiconductor active layer. Similarly, progressive enrichment of one component along the vertical axis of a device, or the presence of a surface wetting layer of one component in a blend, could dramatically impact charge injection/extraction and transport.

While the lateral morphology of polymer blends used in organic electronics has been studied with a variety of techniques,[3−5] only recently has the vertical composition gained more experimental attention.[2,6−9] Vertical phase separation can be promoted by modifying the substrate surface[9−14] or by controlling the solvent evaporation rate.[8,10,15] The vertical composition gradient in the model P3HT:PCBM system has received more limited research. Using variable-angle spectroscopic ellipsometry, Campoy-Quiles et al.[6] reported vertical composition gradients of P3HT:PCBM blends spin coated from chlorobenzene (CB). Blend films on fused silica and poly(3,4-ethylenedioxythiophene) poly(styrenesulfonate) (PEDOT:PSS) substrates generally showed a decreasing PCBM concentration gradient toward the top surface independent of post-treatments (thermal annealing, solvent annealing). When a Si substrate was modified with a hydrophobic self-assembled monolayer, the PCBM concentration gradient could be reversed. The authors concluded that the vertical composition gradient can be tuned by substrate and post-treatment choice. Yamamoto et al. also reported a similar increase of P3HT concentration toward the top surface for P3HT:PCBM films spin coated from chloroform using time-of-flight secondary ion mass spectroscopy (TOF-SIMS).[16] On the other hand, using electron diffraction on blends spin coated from 1,2-dichlorobenzene (ODCB), van Bavel et al.[17,18] reported a bottom interface that was enriched with *crystalline* P3HT for blend films thinner than 200 nm and suggested that the top surface might thus be

Received: November 1, 2010
Accepted: February 8, 2011
Published: March 02, 2011

enriched with PCBM. Potentially, these seemingly disparate concentration gradients could be explained by the different solvents used. P3HT:PCBM organic photovoltaic (OPV) devices from ODCB have been compared to similar devices made from CB by Kim et al.[15] Interestingly, as-fabricated, unannealed devices from ODCB showed more favorable current−voltage characteristics (short-circuit current, fillfactor, and shape) than their unannealed CB counterpart. Kim et al. explained this observation with increased P3HT segregation toward the *bottom* PEDOT:PSS layer for the ODCB devices. Furthermore, thermal annealing of CB made devices improved the device characteristics to be similar to the as-cast ODCB made devices, suggesting that annealing influences the vertical concentration of P3HT in devices processed from CB.[15]

Our group has shown previously that modification of the substrate surface energy by patterning fullerene terminated or carboxylic acid terminated monolayers using dip-pen nanolithography (DPN) and microcontact printing can guide lateral phase separation of polymer:polymer and polymer:fullerene blends with film thicknesses of up to 200 nm,[12,14] with evidence that changes in morphology persist up to the top surface. Using near-edge X-ray absorption fine structure spectroscopy (NEXAFS), Germack et al.[13] reported enrichment of PCBM at the buried interface of high-surface energy SiO_2 and, conversely, P3HT enrichment at the buried interface of samples made on low-surface energy SiO_2 modified with octyltrichlorosilane. They explained this observation with the lower surface energy of P3HT in comparison to PCBM. Similar results, also on Si substrates, have been found by Guan et al.[19] PCBM is the electron-conducting material in P3HT:PCBM OPV devices. Enrichment of PCBM at the electron-collecting electrode is, therefore, beneficial for OPV device performance. While in classical OPV devices the electron-collecting electrode is at the top interface, in inverted OPV structures, it is found at the buried interface between the substrate and active layer. Many groups have recently pursued inverted device architectures. For instance, Hau et al.[20] reported inverted organic solar cells with improved air stability and an electron-collecting electrode of ZnO nanoparticles. Later, they showed that an additional fullerene-based self-assembled monolayer (C_{60}-SAM) between the ZnO layer and the active layer improved device performance of their devices even further, perhaps by improving vertical film morphology.[21] In that study, the authors found evidence that the C_{60} modification to the ZnO preferentially nucleated fullerene on the bottom substrate, but the effects on the composition of the upper surface were not studied. On the basis of the studies described above, it seems possible, even likely, that enrichment of one blend component at one interface due to changes in surface chemistry (or annealing) could lead to corresponding changes at the other interface; however, this possibility has not been studied for functionalized ZnO electrodes.

In this work, we use near-edge X-ray absorption fine structure (NEXAFS) to probe the effects of various substrates and annealing on the top surface-layer composition of polymer blends of regioregular poly-3-hexylthiophene (P3HT) with the fullerene (6,6)-phenyl-C_{61}-butyric acid methyl ester (PCBM) prepared on three chemically distinct substrates that have been used extensively in device applications. To establish a reference point, we use indium tin oxide (ITO)/PEDOT:PSS substrates to study the effect of thermal annealing on classic bulk-heterojunction (BHJ) films prior to cathode deposition. Subsequently, we study the surface composition of P3HT:PCBM blends spin coated onto ITO/ZnO bottom contacts that have been prepared both with and without a C_{60}-SAM interfacial modifier, as have been used in the inverted bulk-heterojunction devices described by Hau et al.[11,20,21]

EXPERIMENTAL METHODS

Sample Preparation. ITO coated glass substrates (Thin Film Devices Inc., Anaheim, CA) were cut to 12 × 12 mm prior to cleaning. After sonication in acetone and isopropanol (15 min each), the substrates were rinsed with IPA and dried under a nitrogen stream. To prepare ITO/PEDOT:PSS substrates, ITO substrates were then air-plasma cleaned (Harrick Plasma PDC-32G, 18 W applied, 5 min cleaning time) and a PEDOT:PSS layer (H.C. Starck CLEVIOS P VP Al 4083, PEDOT:PSS ratio of 1:6, filtered through 0.45 μm PVDF syringe filter, 80 μL, 500 rpm, 30 s; 1750 rpm, 1 min; 5000 rpm, 2 min) was spin coated within 60 s of plasma cleaning. To prepare ITO/ZnO substrates, the ITO was cleaned in the same fashion, after which a ZnO nanoparticle solution was spin coated as described by Hau et al.[20,21]

All spin coating of PEDOT:PSS and ZnO films was performed under ambient conditions. The ITO/PEDOT:PSS substrates were annealed at approximately 100 °C for 30 min under a constant nitrogen stream on a hot plate.

The resulting ITO/PEDOT:PSS and ITO/ZnO substrates were transferred into a dry-nitrogen glovebox (<0.1 ppm H_20, <3 ppm O_2) for further processing. In order to obtain ITO/ZnO/C_{60}-SAM substrates, a C_{60}-SAM solution followed by a pure tetrahydrofuran (THF) solution were each spin coated (50 μL, 3000 rpm, 1 min each) onto the ITO/ZnO samples to form the C_{60}-SAM following protocols described elsewhere.[11,21]

P3HT:PCBM blend (P3HT: average molecular weight 50 000 MW, Sepiolid P100 from Rieke Metals Inc., Lincoln, NE; PCBM: nano-cPCBM-BF from Nano-C Inc., Westwood, MA) solutions (60 mg/mL in chlorobenzene, P3HT:PCBM weight ratios for ITO/PEDOT:PSS and ITO/ZnO substrates are 1:0.95 and 1:0.6, respectively) were stirred overnight at 45 °C. The blend solutions were then filtered (0.2 μm PTFE syringe filter) and spin coated (80 μL, 3000 rpm, 1 min) onto the substrates from a 45 °C warm solution. Sample annealing was performed at 120 °C for 10 min (ITO/PEDOT:PSS/P3HT(1):PCBM(0.95) samples) and 160 °C for 10 min (ITO/ZnO/(C_{60}-SAM)/P3HT(1):PCBM(0.6) samples) to match the protocols for fabrication of working OPV devices made on these electrodes in our laboratories.[21,22] Samples of pure P3HT and PCBM were prepared similarly to the respective blend samples from 30 mg/mL solutions in chlorobenzene. All active layer processing was done in the dry glovebox with minimal light exposure. Pure C_{60} samples were prepared by evaporating a C_{60} film of approximately 50 nm on top of freshly cleaned ITO samples.

NEXAFS Measurements. C *K*-edge NEXAFS measurements of our samples were performed on beamline 8-2 (bending magnet endstation, holographic grating with 500 lines/mm used) at the Stanford Synchrotron Radiation Laboratory (SSRL).[23] A gold grid in the beam path was used for the beam reference measurement. This gold reference grid was freshly sputter-deposited before the measurement run began. The samples were prepared at the University of Washington and transported to SSRL sealed under a nitrogen atmosphere in the dark. Samples were mounted on stainless steel plates with a Ta wire over the samples' top surfaces. During mounting and transferring into the measurement chamber (Stoehr chamber), the samples were exposed to ambient conditions for less than 30 min.

Auger electron yield (AEY) and total electron yield (TEY) measurements over the range of 240−310 eV incident X-ray energy were performed at 55° photon incidence angle (beamline degree of polarization is P = 0.85, corresponding to a magic angle of 51.4°). For AEY measurements, the electron detector (cylindrical mirror analyzer, CMA)

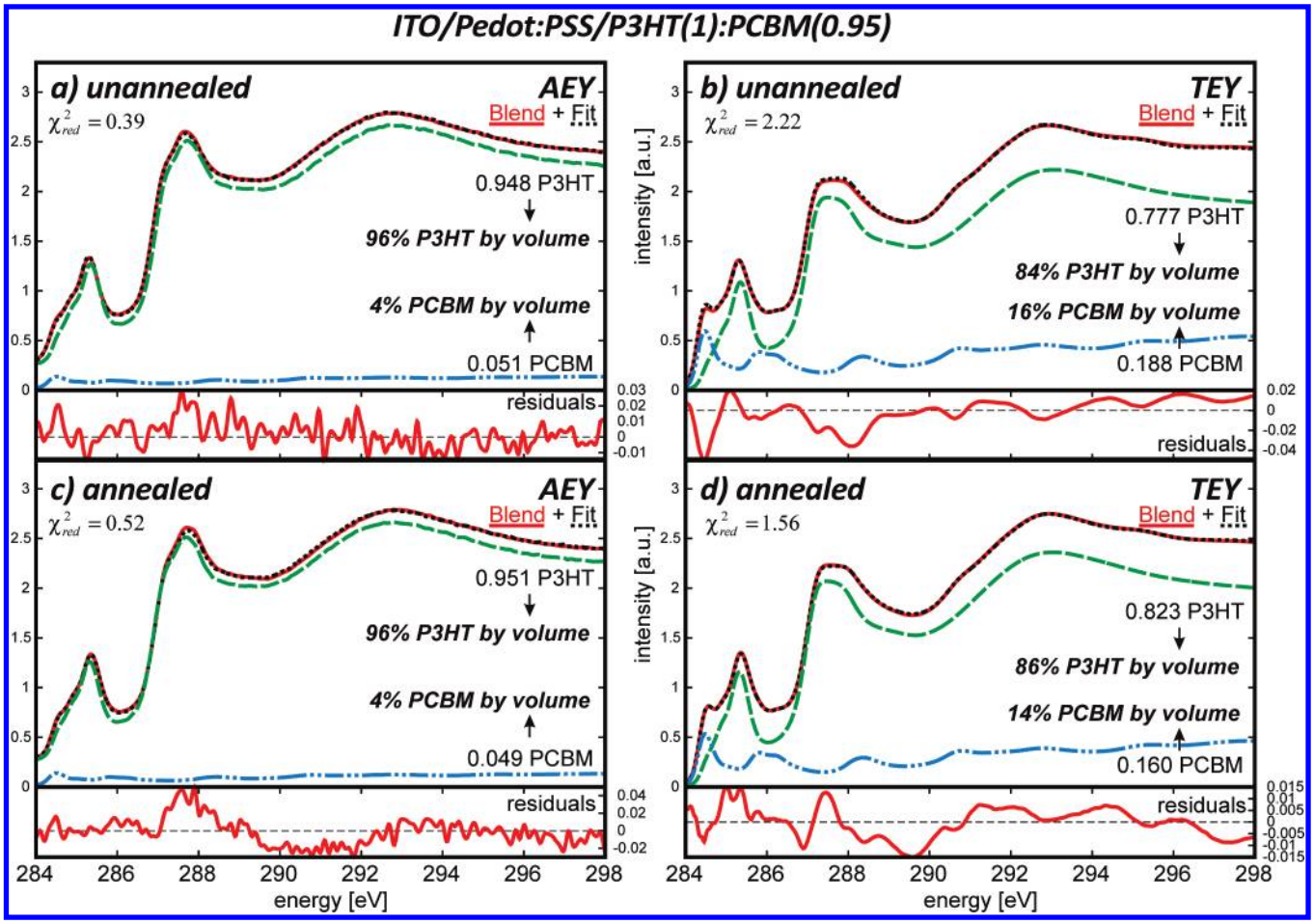

Figure 1. Composition fits on ITO/PEDOT:PSS substrates. Fits and residuals of average P3HT and PCBM spectra (each composed of four individual spectra on two samples) to average ITO/PEDOT:PSS/P3HT(1):PCBM(0.95) blend measurements (each composed of eight individual spectra taken on four samples): (a) AEY measurements on unannealed samples, (b) TEY measurements on unannealed samples, (c) AEY measurements on annealed samples, and (d) TEY measurements on annealed samples.

was set to accept electrons around 257 eV. The raw data was normalized to a gold grid reference measurement[24] taken concurrently and corrected for the linear photoabsorption coefficient of gold.[25] Each spectrum's energy scale was aligned using the first dip in the carbon contamination features of the gold grid reference measurement. An absolute energy scale calibration was performed using the C1s$\rightarrow\pi^*$ peak of highly ordered pyrolytic graphite (HOPG) at 285.38 eV.[26] A pre-edge background was fitted to the pre-edge region up to 284 eV and subtracted from all data. For AEY spectra, a pre-edge background of the form $a/E^3 + b$ was used. For TEY measurements, a constant background plus an exponential decay constraint to reach at most exp(−2) = 13.5% of its initial height (typically, 20% of the constant background) at 280 eV was used. In order to account for experimental variations of the measured signal due to minor misalignments, the average signal from 308 to 309.6 eV of the resulting AEY and TEY spectra was normalized to a constant value. NEXAFS is a 1:1 atomic spectroscopy technique which is sensitive to changes in the atomic environment. This is why proper normalization treatment is important for assigning quantitative compositions in terms of weight or volume (see Supporting Information, SI 1).

Spectra for each individual polymer film were acquired across multiple samples and at different locations on a given sample. A few clear outliers potentially resulting from bad sample wiring were not included in the data analysis. For PCBM, the shape of the reference spectrum was also compared with pure C_{60} and degraded (i.e., intentionally oxidized) PCBM to ensure clean, high-quality spectra (see Supporting Information, SI 3).

Although no problematic beam damage was observed (see Supporting Information, SI 4), in order to minimize spectral changes due to possible beam damage, a new spot on a given sample was used for each individual spectral measurement.

In order to extract the blend composition for each sample type, the linear superposition of average P3HT and PCBM spectra was fit numerically to the average blend measurement. Figures 1 and 2 show the resulting fits with the average spectra used for annealed and unannealed ITO/PEDOT:PSS samples along with the residuals of these fits. Although the magic angle was chosen to minimize angular effects, we cannot exclude that geometrical effects give a small contribution to the residuals at lower energies that might slightly affect the absolute values of the blend ratio.[27] Nevertheless, these uncertainties are small enough that they are unlikely to alter our primary conclusions. The component spectra in these plots have been scaled according to the spectral fractions of their linear superposition as determined by the fits. From these fractions, volume percentages were calculated. Errors for the best-fit fractions were calculated on the basis of investigation of the reduced chi-squared value χ^2_{red} in the parameter space around the best-fit values (see Supporting Information, SI 2).

RESULTS AND DISCUSSION

In light of the differing literature reports on vertical composition gradients measured on P3HT:PCBM blend films via

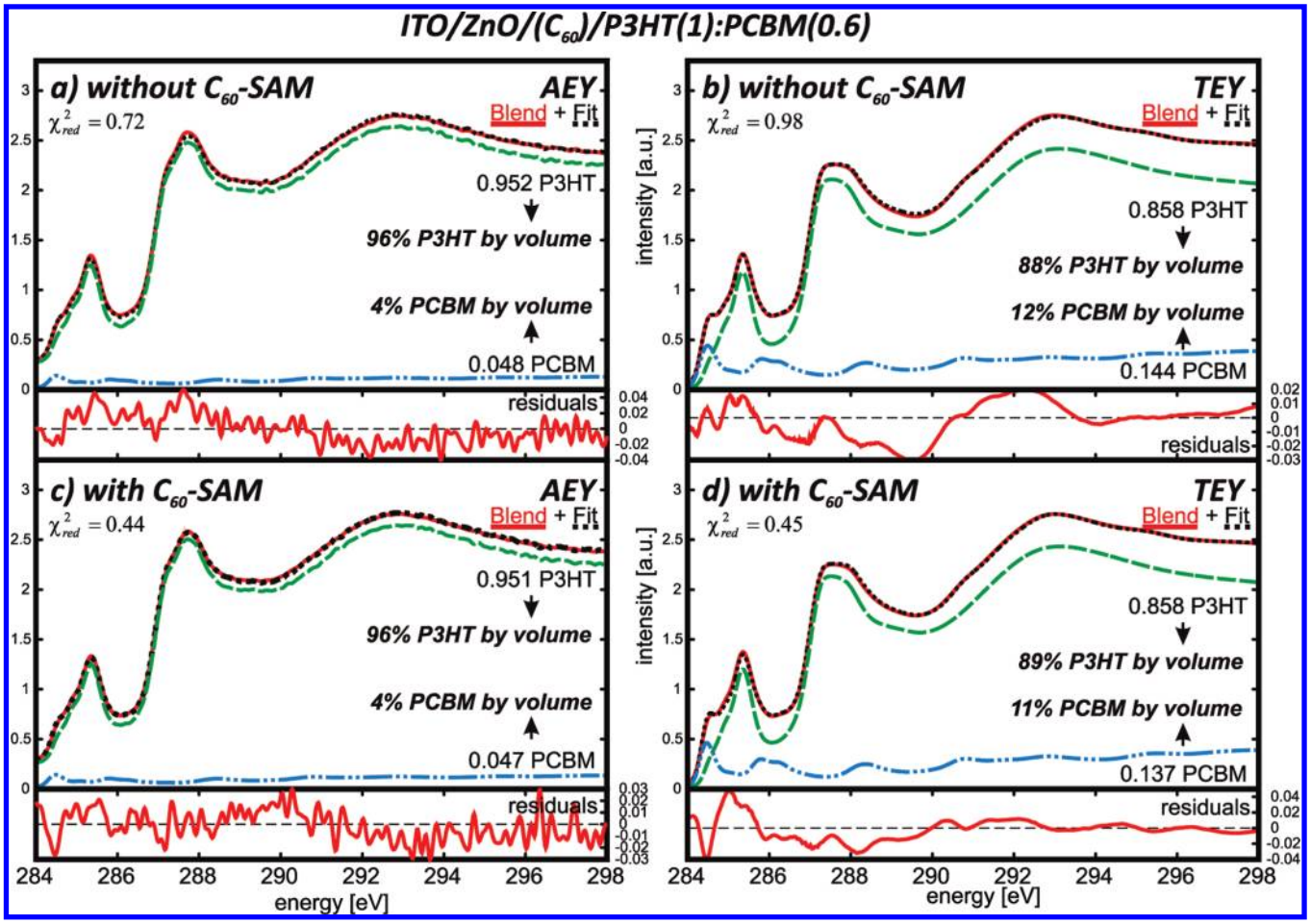

Figure 2. Composition fits on ITO/ZnO substrates. Fits and residuals of P3HT and PCBM spectra to average ITO/ZnO/(C60)/P3HT(1):PCBM(0.6) blend measurements (four individual spectra on two samples for samples without C_{60}-SAM and six spectra on three samples with C_{60}-SAM): (a,b) composition fits on samples without C_{60}-SAM; (c,d) composition fits on samples with C_{60}-SAM.

ellipsometry,[6] electron diffraction,[17] and X-ray photoelectron spectroscopy,[28] as well as prior work in our lab showing that patterned surface chemistry can induce changes in film morphology through the entire vertical structure of the film,[12,14] an important goal of our study is to quantify the material composition of the top layer of device-relevant P3HT:PCBM films. As discussed in the methods section and the Supporting Information, we used the NEXAFS data to determine surface composition of the blends by fitting the blend spectra with linear combinations of the pure P3HT and PCBM spectra, fitting to the respective blend spectrum in the region 284−298 eV. Experimentally, we observed excellent reproducibility of our pure P3HT spectra, which are in good agreement with previous reports.[29−31] The PCBM spectra used in this study were also in good agreement with each other and with the PCBM spectrum recently reported by Germack et al.[13]

ITO/PEDOT:PSS Study. Figure 3a shows the AEY and TEY spectra from blends of P3HT:PCBM (1:0.95 weight ratio) spin coated onto ITO/PEDOT:PSS substrates both with and without thermal annealing treatment. The AEY spectra overlap perfectly within the measurement uncertainty and closely resemble the AEY spectra of pure P3HT films, suggesting that the uppermost film surface (∼1−2 nm) is almost entirely P3HT. On the other hand, the TEY spectra both before and after annealing appear to contain more contribution from PCBM (features around 284.5 and 286.0 eV) than the AEY spectra. Furthermore, unlike the AEY spectra, the TEY spectra show a small but reproducible evolution after annealing: the annealed samples exhibit a slightly higher peak at 287.5 eV. This larger peak is at the same energy as the σ^*(C−S/C−H) transition[30,32] and indicates slightly higher P3HT content in the TEY spectra after annealing. For our AEY spectra, the fit residuals are very small, of comparable magnitude to the blend films′ standard deviations. Since the NEXAFS bandshapes for polythiophenes are known to be very sensitive to the local environment,[33] this suggests that the local environment (i.e., π-stacking of P3HT) between blend and single component films are nearly identical. The excellent agreement between the AEY spectrum in the blend and the single-component P3HT films is, thus, further evidence for the formation of a complete P3HT wetting layer at the surface. We believe that the spectral variations in the TEY spectra upon annealing are mainly due to a change in blend composition because the fit residuals around the σ^*(C−S/C−H) transition as well as the differences between annealed and unannealed P3HT spectra are within the blend's measurement uncertainties. However, the slightly worse residuals in the TEY fits could also arise from a subtly different molecular environment for some P3HT chains as well as orientational changes of P3HT in the subsurface region where PCBM is present. Furthermore, the minor fit overshoot around 284.5 eV in the region of the π^*(C═C) transition of the PCBM's

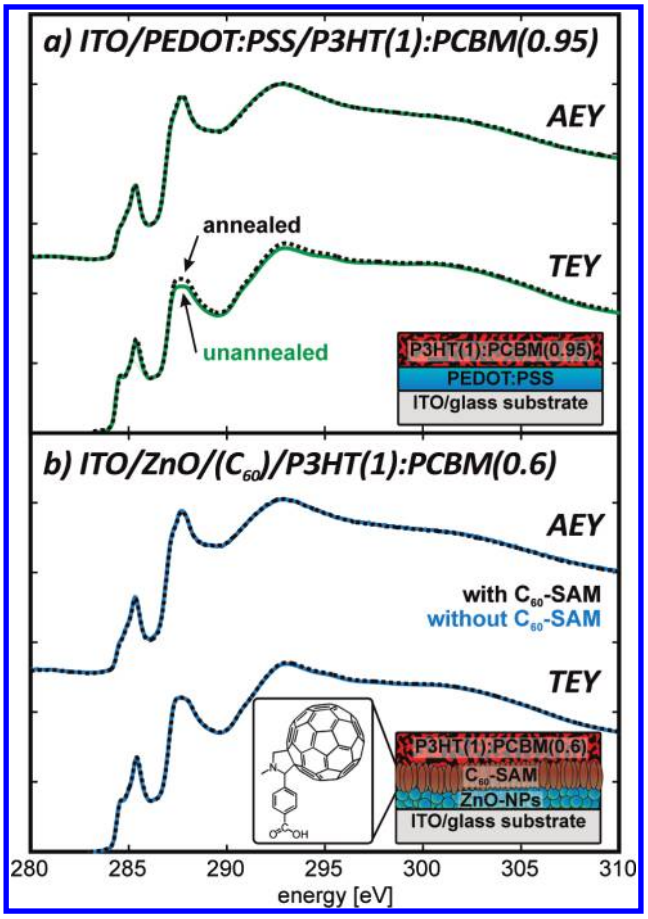

Figure 3. Blend measurements on ITO/PEDOT:PSS and ITO/ZnO samples. AEY and TEY blend averages of (a) ITO/PEDOT:PSS/P3HT(1):PCBM(0.95) (each average is composed of eight individual spectra taken on four samples) and (b) ITO/ZnO/(C_{60}-SAM)/P3HT-(1):PCBM(0.6) (four individual spectra on two samples without C_{60}-SAM, five individual spectra on three samples with C_{60}-SAM); with or without the additional C_{60}-SAM, the spectra overlap within measurement error.

fullerene cage could indicate slight changes of the fullerene cage in the blend compared to single component PCBM.

When analyzed quantitatively, the AEY and TEY spectra provide important complementary information about the different vertical profiles of P3HT and PCBM at the film surface. The AEY measurements are more surface sensitive than TEY measurements. The mean free path of Auger electrons detected in an AEY measurement governs its sampling depth which is on the order of 1−2 nm for C Auger electrons.[24] On the other hand, the sampling depth of the TEY measurements is determined by the electron escape depth, which is somewhat deeper. Classic continuum estimates of the TEY sensitivity depth are ∼10 nm,[24] but recent work by Chua et al.[34] suggests a much smaller depth of 2−3 nm in P3HT films. The exact value of the TEY escape length has only a minor influence on our composition results, altering the distance over which the wetting layer evolves (but never reaches) the bulk. For brevity in the subsequent discussion, we adopt the value of 2−3 nm after Chua et al.[34] With this information and composition fits as shown in Figure 1a−d and summarized in Table 1, we can form a more detailed picture of the P3HT:PCBM blend surface region. Since the AEY data show that the film composition is at most 4% PCBM in the top ∼1−2 nm, we conclude that P3HT forms a nearly complete wetting layer on P3HT:PCBM blend films spin coated from chlorobenzene with only a few PCBM clusters penetrating the topmost surface region. This conclusion is in good agreement with the results of Germack et al.[35] obtained by NEXAFS and Xu et al.[28] obtained by XPS and could also be consistent with the model obtained by Campoy-Quiles et al.[6] through fits to ellipsometry data. On the other hand, our results appear less consistent with suggestions of a PCBM rich top surface reported by van Bavel et al.[17,18] and Kim et al.[15] for devices made from ODCB based on measurements made with ellipsometry and are inconsistent with the ultrathin PCBM overlayer that was proposed by Spadafora et al.[36] on the basis of Kelvin probe imaging.

Going slightly deeper into the film, our TEY data show that before annealing, the top ∼2−3 nm of the film contains a significantly higher percentage of PCBM (16%) than the topmost ∼1−2 nm probed by AEY. Nevertheless, this concentration is still well below the expected volume percentage of PCBM (∼50% by volume, based on P3HT and PCBM densities according to Supporting Information, SI 1) in the overall bulk of the film. The observed depletion of PCBM in the top-layer of our P3HT:PCBM samples in conjunction with the reproducibility of this observation across different locations on multiple samples seems to confirm that P3HT intrinsically prefers the film−air interface due to a lower surface energy. Any surface-directed phase separation would be further amplified by thermal annealing, after which the PCBM concentration in the top ∼2−3 nm surface region decreases by a small but measurable amount in all samples, going from 16% to 14%. Surface-directed spinodal decomposition was previously reported for different polymer systems[9,37,38] and could provide one possible mechanism of self-stratification. The top surface is where the electron-collecting electrode is deposited in a classical BHJ OPV device architecture, and since P3HT is the hole transport layer in these devices, high P3HT content near the electron-collecting electrode could be detrimental to device performance unless the contact metallization step significantly penetrated the surface P3HT layer. The observed phase separation of the high surface-energy phase away from the top surface during solvent evaporation while spin coating and also during thermal annealing could be used to incorporate additional layers into a pre-existing film morphology, thereby controlling vertical morphology. For example, improved device performance compared to regular P3HT:PCBM BHJ OPV devices has been shown for P3HT:PCBM devices with an additional PCBM layer on top by Kumar et al.[39] and de Villers et al.[40] or an additional P3HT layer at the substrate interface by Liang et al.[41] Likewise, increased performance compared to regular P3HT:PCBM devices was reported by Wang et al.[42] for P3HT-rich bottom/PCBM-rich top bilayer devices with an observed concentration gradient between both layers.

ITO/ZnO Study. While the P3HT:PCBM samples spin coated onto ITO/PEDOT:PSS substrates provide useful information about vertical stratification and the effects of annealing on model device structures, an important goal of this study is to examine the effects of buried substrate chemistry on the top film surface composition. In other words, can the bottom substrate effects penetrate all the way to the top surface in these films? Figure 3b shows both AEY and TEY NEXAFS spectra taken on annealed P3HT:PCBM (1:0.6 weight ratio) blends spin coated onto substrates identical to those that have been used to fabricate previously reported inverted OPV devices:[11,21] specifically ZnO films deposited from colloidal ZnO suspensions and either

Table 1. Blend Composition Fit Results

substrate	AEY P3HT:PCBM	AEY PCBM fraction[a]	TEY P3HT:PCBM	TEY PCBM fraction[a]
ITO/PEDOT:PSS unannealed	96:4%	4.1 ± 3.3 (2.4)%	84:16%	16.3 ± 1.5 (1.1)%
ITO/PEDOT:PSS annealed	96:4%	3.9 ± 3.1 (2.2)%	86:14%	13.6 ± 1.2 (0.9)%
ZnO annealed	96:4%	3.8 ± 2.7 (2.0)%	88:12%	11.9 ± 0.7 (0.5)%
ZnO/C_{60}-SAM annealed	96:4%	3.8 ± 1.8 (1.3)%	89:11%	11.4 ± 1.6 (1.1)%

[a] Errors are for 90% (68%) confidence interval as described in Supporting Information, SI2.

functionalized with a C_{60}-SAM layer or left as bare ZnO. The spectra of the two systems with and without the C_{60}-SAM underneath the film are identical. These identical spectra are observed for AEY as well as TEY measurements. We thus conclude that the presence of the C_{60}-SAM on the bottom electrode does not have a significant influence on the top surface composition: for the films studied here, the P3HT top-surface wetting layer is always present, and the PCBM concentration near the film−air interface is not measurably affected by the presence of the buried C_{60}-SAM.

The quantitative values of PCBM concentration near the top surface in the blends on the ZnO samples also provide new data about vertical morphology on these substrates. As summarized in Table 1 (composition fits in Supporting Information, SI2), the AEY PCBM concentration in the top ∼1−2 nm is approximately 4%, again consistent with the presence of a P3HT wetting layer at the film/air interface. The PCBM concentration measured using TEY is around 11−12% (similar within uncertainty) or about one-quarter of the expected bulk volume percentage (∼40% PCBM by volume in stock solution). The amount of PCBM seen in the TEY measurements on the ZnO samples deposited from 1:0.6 P3HT:PCBM blends is *lower* than the PCBM concentration seen in the TEY measurements on samples deposited from 1:0.95 P3HT:PCBM blends on ITO/PEDOT:PSS. In relation to the stock solution concentrations, however, the observed PCBM concentrations are approximately one-quarter of the expected bulk concentrations in both our ZnO and ITO/PEDOT:PSS samples (∼40% and ∼50% PCBM by volume, respectively). This result indicates that the concentration of PCBM in the top ∼2−3 nm is weakly influenced by the ratio of P3HT:PCBM in the stock solution and that the sample is just beginning to approach the "bulk" solution composition over the sample depth of the TEY (∼2−3 nm) measurement.

CONCLUSIONS

In conclusion, we have used NEXAFS AEY measurements to show that the top surface layer (∼1−2 nm) of P3HT:PCBM blend films on substrates of both ITO/PEDOT:PSS and ITO/ZnO (with or without a C_{60}-SAM) consists almost exclusively of P3HT. The existence of this molecular wetting layer is further supported by the fact that the TEY measurements which should probe the top 2−3 nm in P3HT[34] still showed lower PCBM concentrations than expected for the bulk, evidencing that the TEY measurement did not reach the bulk. However, the PCBM volume fraction measured in the top ∼3 nm as deduced from TEY is still weakly influenced by the ratio of P3HT:PCBM in the stock solution, suggesting that the film begins returning to a more bulklike composition over this distance. We also found that annealing blend films at 120 °C for 10 min on ITO/PEDOT:PSS substrates slightly lowers the PCBM concentration in the immediate subsurface (∼2−3 nm) region by approximately 20% (relative), which we attribute to improved coverage of the P3HT surface wetting layer. On ITO/ZnO substrates, we observed no change in the fractional top surface composition of the P3HT(1):PCBM(0.6) blends whether a C_{60}-SAM was present to modify the bottom ZnO/polymer interface or not. For the approximately 150 nm thick, devicelike films studied here, the total fraction of PCBM in the top ∼2−3 nm of the film appears fairly insensitive to the buried surface chemistry.

The reported values are for the free surface; the effects of thermal annealing on the vertical structure in a completed BHJ-OPV device are likely dependent on the metal surface layer used. A number of studies have now reported seemingly conflicting results for the top surface composition of P3HT:PCBM blend films.[13,16−19,28,35,40,43−46] While materials and preparation conditions may explain some of the reported variation in top surface composition, our results are consistent with P3HT wetting layers being present at the top surface of films on a range of different substrates, under a range of annealing conditions. We note that, including this experiment, most reports of which we are currently aware[13,19,28,35,45−47] using direct spectroscopic measurements (NEXAFS and XPS) sensitive to thin surface layers have found a P3HT-rich surface. Given the indirect nature of inferring vertical composition involved with some other methods, we thus conclude that a thin P3HT surface layer is likely a general feature of P3HT:PCBM blends due to the lower surface energy of P3HT.[13,19]

If this surface layer is indeed driven by the interfacial energies of P3HT:PCBM, then this material system would naturally favor vertical phase separation (at least at that top surface) that is more favorable to inverted diode structures. Likewise, intentional control of the relative surface energies of the donor and acceptor phases used in OPVs via chemical derivatization or inclusion of surface wetting agents could be used to achieve better electron/hole blocking layers in devices.

ASSOCIATED CONTENT

Supporting Information. Detailed information about the data normalization (including a calculation of the density of PCBM), the fit model, and the error estimation as well as a comparison of PCBM to C_{60} spectra and beam damage evaluation. This material is available free of charge via the Internet at http://pubs.acs.org.

AUTHOR INFORMATION

Corresponding Author
*E-mail: ginger@chem.washington.edu.

ACKNOWLEDGMENT

This paper is based on work supported by the Department of Energy Solar America Initiative. Portions of this research were carried out at the Stanford Synchrotron Radiation Laboratory, a

national user facility operated by Stanford University on behalf of the U.S. Department of Energy, Office of Basic Energy Sciences. D.S.G. thanks the Research Corporation Cottrell Scholars Program, Alfred P. Sloan Foundation Fellowship Program, and Camille Dreyfus Teacher-Scholar Program for additional support. K.M.N. acknowledges partial support from an IGERT Fellowship Award und NSF DGE-050457 at the Center for Nanotechnology at the UW. B.A.M. performed this research as a NSF Graduate Research Fellow. G.T.S. acknowledges support from the U.S. Department of Energy, Basic Energy Sciences. We thank Dr. Dean M. DeLongchamp (NIST) and Dr. Bryant Fujimoto (UW) for valuable input regarding data analysis.

REFERENCES

(1) Chen, L. M.; Xu, Z.; Hong, Z. R.; Yang, Y. *J. Mater. Chem.* **2010**, *20*, 2575–2598.
(2) Giridharagopal, R.; Ginger, D. S. *J. Phys. Chem. Lett.* **2010**, *1*, 1160–1169.
(3) Erb, T.; Zhokhavets, U.; Gobsch, G.; Raleva, S.; Stuhn, B.; Schilinsky, P.; Waldauf, C.; Brabec, C. J. *Adv. Funct. Mater.* **2005**, *15*, 1193–1196.
(4) Ma, W. L.; Yang, C. Y.; Gong, X.; Lee, K.; Heeger, A. J. *Adv. Funct. Mater.* **2005**, *15*, 1617–1622.
(5) Benanti, T. L.; Venkataraman, D. *Photosynth. Res.* **2006**, *87*, 73–81.
(6) Campoy-Quiles, M.; Ferenczi, T.; Agostinelli, T.; Etchegoin, P. G.; Kim, Y.; Anthopoulos, T. D.; Stavrinou, P. N.; Bradley, D. D. C.; Nelson, J. *Nat. Mater.* **2008**, *7*, 158–164.
(7) Geoghegan, M.; Krausch, G. *Prog. Polym. Sci.* **2003**, *28*, 261–302.
(8) Walheim, S.; Boltau, M.; Mlynek, J.; Krausch, G.; Steiner, U. *Macromolecules* **1997**, *30*, 4995–5003.
(9) Jones, R. A. L.; Norton, L. J.; Kramer, E. J.; Bates, F. S.; Wiltzius, P. *Phys. Rev. Lett.* **1991**, *66*, 1326–1329.
(10) Arias, A. C.; Corcoran, N.; Banach, M.; Friend, R. H.; MacKenzie, J. D.; Huck, W. T. S. *Appl. Phys. Lett.* **2002**, *80*, 1695–1697.
(11) Hau, S. K.; Yip, H. L.; Acton, O.; Baek, N. S.; Ma, H.; Jen, A. K. Y. *J. Mater. Chem.* **2008**, *18*, 5113–5119.
(12) Park, L. Y.; Munro, A. M.; Ginger, D. S. *J. Am. Chem. Soc.* **2008**, *130*, 15916–15926.
(13) Germack, D. S.; Chan, C. K.; Hamadani, B. H.; Richter, L. J.; Fischer, D. A.; Gundlach, D. J.; DeLongchamp, D. M. *Appl. Phys. Lett.* **2009**, *94*, 233303.
(14) Coffey, D. C.; Ginger, D. S. *J. Am. Chem. Soc.* **2005**, *127*, 4564–4565.
(15) Kim, Y.; Choulis, S. A.; Nelson, J.; Bradley, D. D. C.; Cook, S.; Durrant, J. R. *Appl. Phys. Lett.* **2005**, *86*, 063502.
(16) Yamamoto, S.; Kitazawa, D.; Tsukamoto, J.; Shibamori, T.; Seki, H.; Nakagawa, Y. *Thin Solid Films* **2010**, *518*, 2115–2118.
(17) van Bavel, S.; Sourty, E.; de With, G.; Frolic, K.; Loos, J. *Macromolecules* **2009**, *42*, 7396–7403.
(18) van Bavel, S. S.; Sourty, E.; de With, G.; Loos, J. *Nano Lett.* **2009**, *9*, 507–513.
(19) Guan, Z.-L.; Kim, J. B.; Wang, H.; Jaye, C.; Fischer, D. A.; Loo, Y.-L.; Kahn, A. *Org. Electron.* **2010**, *11*, 1779–1785.
(20) Hau, S. K.; Yip, H. L.; Baek, N. S.; Zou, J. Y.; O'Malley, K.; Jen, A. K. Y. *Appl. Phys. Lett.* **2008**, *92*, 253301.
(21) Hau, S. K.; Yip, H. L.; Ma, H.; Jen, A. K. Y. *Appl. Phys. Lett.* **2008**, *93*, 253301.
(22) Pingree, L. S. C.; Reid, O. G.; Ginger, D. S. *Nano Lett.* **2009**, *9*, 2946–2952.
(23) Tirsell, K. G.; Karpenko, V. P. *Nucl. Instrum. Methods A* **1990**, *291*, 511–517.
(24) Stoehr, J. In *NEXAFS spectroscopy*; Springer-Verlag: Berlin and New York, 1992.
(25) Watts, B.; Thomsen, L.; Dastoor, P. C. *J. Electron Spectrosc. Relat. Phenom.* **2006**, *151*, 105–120.
(26) Batson, P. E. *Phys. Rev. B: Condens. Matter Mater. Phys.* **1993**, *48*, 2608–2610.
(27) Xue, B.; Vaughan, B.; Poh, C.-H.; Burke, K. B.; Thomsen, L.; Stapleton, A.; Zhou, X.; Bryant, G. W.; Belcher, W.; Dastoor, P. C. *J. Phys. Chem. C* **2010**, *114*, 15797–15805.
(28) Xu, Z.; Chen, L. M.; Yang, G. W.; Huang, C. H.; Hou, J. H.; Wu, Y.; Li, G.; Hsu, C. S.; Yang, Y. *Adv. Funct. Mater.* **2009**, *19*, 1227–1234.
(29) Kim, D. H.; Jang, Y.; Park, Y. D.; Cho, K. *Langmuir* **2005**, *21*, 3203–3206.
(30) DeLongchamp, D. M.; Lin, E. K.; Fischer, D. A. *Proc. SPIE* **2005**, *5940*, 59400A.
(31) Gurau, M. C.; Delongchamp, D. M.; Vogel, B. M.; Lin, E. K.; Fischer, D. A.; Sambasivan, S.; Richter, L. J. *Langmuir* **2007**, *23*, 834–842.
(32) Stoehr, J.; Gland, J. L.; Kollin, E. B.; Koestner, R. J.; Johnson, A. L.; Muetterties, E. L.; Sette, F. *Phys. Rev. Lett.* **1984**, *53*, 2161–2164.
(33) Ho, P. K. H.; Chua, L. L.; Dipankar, M.; Gao, X. Y.; Qi, D. C.; Wee, A. T. S.; Chang, J. F.; Friend, R. H. *Adv. Mater. (Weinheim, Ger.)* **2007**, *19*, 215–221.
(34) Chua, L. L.; Dipankar, M.; Sivaramakrishnan, S.; Gao, X. Y.; Qi, D. C.; Wee, A. T. S.; Ho, P. K. H. *Langmuir* **2006**, *22*, 8587–8594.
(35) Germack, D. S.; Chan, C. K.; Kline, R. J.; Fischer, D. A.; Gundlach, D. J.; Toney, M. F.; Richter, L. J.; DeLongchamp, D. M. *Macromolecules* **2010**, *43*, 3828–3836.
(36) Spadafora, E. J.; Demadrille, R.; Ratier, B.; Grévin, B. *Nano Lett.* **2010**, *10*, 3337–3342.
(37) Budkowski, A.; Bernasik, A.; Cyganik, P.; Rysz, J.; Brenn, R. *e-Polym.* **2002**, 006 (article number).
(38) Han, X.; Liu, H. L.; Hu, Y. *J. Polym. Sci., Part B: Polym. Phys.* **2007**, *45*, 532–543.
(39) Kumar, A.; Li, G.; Hong, Z. R.; Yang, Y. *Nanotechnology* **2009**, *20*, 165202.
(40) de Villers, B. T.; Tassone, C. J.; Tolbert, S. H.; Schwartz, B. J. *J. Phys. Chem. C* **2009**, *113*, 18978–18982.
(41) Liang, C. W.; Su, W. F.; Wang, L. Y. *Appl. Phys. Lett.* **2009**, *95*, 133303.
(42) Wang, D. H.; Choi, D. G.; Park, O. O.; Park, J. H. *J. Mater. Chem.* **2010**, *20*, 4910–4915.
(43) Yang, X. N.; Loos, J.; Veenstra, S. C.; Verhees, W. J. H.; Wienk, M. M.; Kroon, J. M.; Michels, M. A. J.; Janssen, R. A. J. *Nano Lett.* **2005**, *5*, 579–583.
(44) Parnell, A. J.; Dunbar, A. D. F.; Pearson, A. J.; Staniec, P. A.; Dennison, A. J. C.; Hamamatsu, H.; Skoda, M. W. A.; Lidzey, D. G.; Jones, R. A. L. *Adv. Mater. (Weinheim, Ger.)* **2010**, *22*, 2444–2447.
(45) Orimo, A.; Masuda, K.; Honda, S.; Benten, H.; Ito, S.; Ohkita, H.; Tsuji, H. *Appl. Phys. Lett.* **2010**, *96*, 043305.
(46) Xu, Z.; Chen, L. M.; Chen, M. H.; Li, G.; Yang, Y. *Appl. Phys. Lett.* **2009**, *95*, 013301.
(47) Qiu, L.; Lim, J. A.; Wang, X.; Lee, W. H.; Hwang, M.; Cho, K. *Adv. Mater. (Weinheim, Ger.)* **2008**, *20*, 1141–1145.